

# One-Step Synthesis and Schlenk-Type Equilibrium of Cyclopentadienylmagnesium Bromides

Philipp Schüler,<sup>[a]</sup> Helmar Görls,<sup>[a]</sup> Sven Krieck,<sup>[a]</sup> and Matthias Westerhausen<sup>\*[a]</sup>

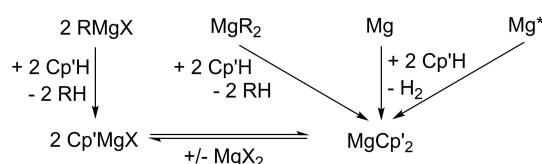
**Abstract:** In the in situ Grignard metalation method (iGMM), the addition of bromoethane to a suspension of magnesium turnings and cyclopentadienes [C<sub>5</sub>H<sub>6</sub> (HCp), C<sub>5</sub>H<sub>5</sub>-Si(iPr)<sub>3</sub> (HCp<sup>TIP5</sup>)] in diethyl ether smoothly yields heteroleptic [(Et<sub>2</sub>O)Mg(Cp<sup>R</sup>)(μ-Br)]<sub>2</sub> (Cp<sup>R</sup>=Cp (1), Cp<sup>TIP5</sup> (2)). The Schlenk equilibrium of 2 in toluene leads to ligand exchange and formation of homoleptic [Mg(Cp<sup>R</sup>)<sub>2</sub>] (3) and [(Et<sub>2</sub>O)MgBr(μ-Br)]<sub>2</sub> (4). Interfering solvation and aggregation as well as ligand redistribution equilibria hamper a quantitative elucidation of

thermodynamic data for the Schlenk equilibrium of 2 in toluene. In ethereal solvents, mononuclear species [(Et<sub>2</sub>O)<sub>n</sub>Mg(Cp<sup>TIP5</sup>)Br] (2'), [(Et<sub>2</sub>O)<sub>n</sub>Mg(Cp<sup>TIP5</sup>)<sub>2</sub>] (3'), and [(Et<sub>2</sub>O)<sub>2</sub>MgBr<sub>2</sub>] (4') coexist. Larger coordination numbers can be realized with cyclic ethers like tetrahydropyran allowing crystallization of [(thp)<sub>4</sub>MgBr<sub>2</sub>] (5). The interpretation of the temperature-dependency of the Schlenk equilibrium constant in diethyl ether gives a reaction enthalpy ΔH and reaction entropy ΔS of -11.5 kJ mol<sup>-1</sup> and 60 J mol<sup>-1</sup>, respectively.

## Introduction

Magnesocene (MgCp<sub>2</sub>) [and also its substituted derivatives (MgCp'<sub>2</sub>)<sup>[1]</sup>] are very stable molecules that are available via direct metalation of cyclopentadiene (HCp) with activated magnesium Mg\* or magnesium turnings under drastic reaction conditions or via metalation of CpH with alkylmagnesium reagents (Scheme 1).<sup>[2,3]</sup> The latter pathway requires the synthesis of Grignard reagents and subsequently the metalation reaction. Alternatively, activation of Mg is possible to perform the preparation of magnesocenes under common mild metal-organic reaction conditions. The magnesocene complexes react violently with water and show comparable <sup>13</sup>C NMR shifts as observed for the alkali metal cyclopentadienides suggesting an essentially ionic Mg–Cp interaction. Furthermore, MgCp<sub>2</sub> shows low conductivity in ethereal solutions which confirms dissociation in these solvents and - contrary to classical Grignard solutions<sup>[4]</sup> - a sufficient anodic stability limit to be considered as an electrolyte for nonaqueous magnesium-based batteries.<sup>[5]</sup>

Detailed investigation of the donor influence on the chemical <sup>25</sup>Mg and <sup>13</sup>C NMR shifts of magnesocene suggests complexation with diethyl ether as well as tetrahydrofuran.<sup>[6]</sup> It is noteworthy that the <sup>25</sup>Mg shifts strongly depend on the molar ratio of MgCp<sub>2</sub> to THF and a constant chemical shift has been



**Scheme 1.** Simplified reaction pathways for the synthesis of magnesocenes (Mg\* = activated magnesium like Rieke magnesium, Cp' = substituted or unsubstituted cyclopentadienyl).

observed if more than three equivalents of THF have been added to magnesocene. An equilibrium between [(thf)<sub>2</sub>MgCp<sub>2</sub>] and THF on the one side and [(thf)<sub>3</sub>MgCp<sub>2</sub>] on the other has been concluded.

The reaction of RMgX with HCp' yields RH and half-sandwich complexes Cp'MgX stabilized by electroneutral Lewis bases. Depending on the donor strength and the bulkiness of the coligands and of the Cp' anions, mononuclear complexes or dinuclear molecules with bridging halide ions have been isolated; representative examples are for example [(Me<sub>3</sub>Si)<sub>3</sub>C<sub>5</sub>H<sub>2</sub>]Mg(tmeda)Br<sup>[7]</sup> from MgMe<sub>2</sub> and (Me<sub>3</sub>Si)<sub>3</sub>C<sub>5</sub>H<sub>3</sub> as well as [Cp'Mg(thf)(μ-Br)]<sub>2</sub> (Cp' = C<sub>5</sub>Me<sub>4</sub>H, Cp\*) as by-products during the synthesis of sterically protected aluminum clusters.<sup>[8]</sup> Furthermore, the molecular structures of [CpMg(Py)(μ-Br)]<sub>2</sub><sup>[9]</sup> and [(Cp\*)Mg(Dmf)(μ-Br)]<sub>2</sub><sup>[10]</sup> have been reported. Comparable dimeric structures have also been observed for the chloro complexes [CpMg(OEt<sub>2</sub>)(μ-Cl)]<sub>2</sub> and [(Cp\*)Mg(OEt<sub>2</sub>)(μ-Cl)]<sub>2</sub>.<sup>[11]</sup>

Heteroleptic CpMgBr can undergo Schlenk-type ligand redistribution reactions yielding homoleptic magnesocene and MgBr<sub>2</sub> according to Scheme 1.<sup>[2]</sup> The coordination chemistry of MgBr<sub>2</sub> in ethereal solvents is surprisingly complex, depending on donor strength as well as isolation and crystallization conditions. Thus, various species derived from magnesium bromide in THF solution are known, not only including the electroneutral thf adducts [(thf)<sub>2</sub>MgBr<sub>2</sub>]<sub>∞</sub><sup>[12]</sup> [(thf)<sub>3</sub>MgBr<sub>2</sub>]<sup>[13]</sup> and

[a] P. Schüler, Dr. H. Görls, Dr. S. Krieck, Prof. Dr. M. Westerhausen  
Institute of Inorganic and Analytical Chemistry  
Friedrich Schiller University Jena  
Humboldtstraße 8, 07743 Jena (Germany)  
E-mail: m.we@uni-jena.de

Supporting information for this article is available on the WWW under <https://doi.org/10.1002/chem.202102636>

© 2021 The Authors. Chemistry - A European Journal published by Wiley-VCH GmbH. This is an open access article under the terms of the Creative Commons Attribution Non-Commercial NoDerivs License, which permits use and distribution in any medium, provided the original work is properly cited, the use is non-commercial and no modifications or adaptations are made.

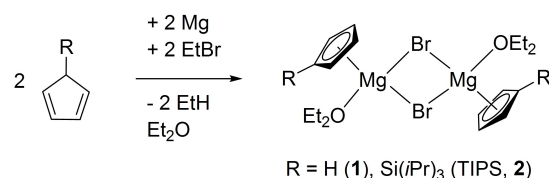
[(thf)<sub>4</sub>MgBr<sub>2</sub>]<sup>[14]</sup> but also ionic derivatives such as [(thf)<sub>5</sub>MgBr]<sup>+ [15]</sup> as well as anionic [(thf)MgBr<sub>3</sub>]<sup>- [16]</sup> and [MgBr<sub>4</sub>]<sup>2- [17]</sup>. Variation of the coordination number of magnesium can also be expected for diethyl ether adducts. However, up to now, only the structural parameters of mononuclear [(Et<sub>2</sub>O)<sub>2</sub>MgBr<sub>2</sub>] are available.<sup>[18]</sup>

Solvation of magnesocenes have to be taken into account, too. Structurally authenticated thf adducts are [(thf)MgCp<sub>2</sub>]<sup>[19]</sup> and [(thf)<sub>2</sub>MgCp<sub>2</sub>]<sup>[20]</sup> with an increasing slippage of the Cp ring from η<sup>5</sup>- to η<sup>1</sup>-coordination with increasing number of ligated bases. Stronger bases such as dimethylsulfoxide (dmsO) are even able to stabilize solvent-separated ion pairs [Mg(dmsO)<sub>6</sub>]<sup>2+</sup> 2[Cp<sup>-</sup>].<sup>[20]</sup> For bulkier bis(indenyl)magnesium the thf base is already strong enough to build comparable solvent-separated ions [Mg(thf)<sub>6</sub>]<sup>2+</sup> 2[Ind<sup>-</sup>].<sup>[21]</sup> Further enhancement of the aromatic system further weakens the interactions with magnesium ions and bis(fluorenyl)magnesium crystallizes as bis(diethyl ether) adduct [(Et<sub>2</sub>O)<sub>2</sub>Mg(Flu)<sub>2</sub>].<sup>[22]</sup> In addition, bulky substituents cannot prevent adduct formation and hence, [(thf)<sub>2</sub>Mg{C<sub>5</sub>H<sub>4</sub>-P(*i*Pr)<sub>2</sub>}]<sub>2</sub> precipitates as a bis(thf) complex with η<sup>5</sup>- and η<sup>2</sup>-bonded diisopropylphosphanyl cyclopentadienyl ligands.<sup>[23]</sup>

In this study an improved straightforward synthesis of cyclopentadienyl magnesium bromides in ethereal solvents is presented by transferring the in situ Grignard metalation method (iGMM) to this compound class; so far this process has only been established for the synthesis of Mg{N(SiMe<sub>3</sub>)<sub>2</sub>}.<sup>[24]</sup> Furthermore, the elucidation of thermodynamic data of the temperature-dependent Schlenk equilibrium is reported.

## Results and Discussion

On the one hand, commercially available magnesium is unable to deprotonate cyclopentadiene under common organometallic reaction conditions but temperatures of approx. 500 °C enable the formation of magnesocene. On the other hand, activation of magnesium via for example the Rieke method (reduction of magnesium halide with potassium) yields pyrophoric magnesium powder that poses an additional hazard for a reaction in diethyl ether. In order to circumvent these challenges, we developed the in situ Grignard metalation method (iGMM), a one-pot synthesis for the preparation of Mg{N(SiMe<sub>3</sub>)<sub>2</sub>}.<sup>[24]</sup> In analogy to this procedure, Mg turnings and cyclopentadiene (HCp) were suspended in an ethereal solvent and bromoethane was added at 0 °C within 30 minutes. Then the reaction mixture was warmed to room temperature and decanted from excess of magnesium. Storage of this reaction solution at room temperature for two days yielded large colorless crystals of [(Et<sub>2</sub>O)MgCp(μ-Br)]<sub>2</sub> (1). Diethyl ether was the preferred solvent because crystalline products could easily be isolated. In THF solution, the reaction proceeded similarly, however, oily [(thf)<sub>n</sub>MgCpBr] with varying thf content formed and crystallization of a pure compound failed. The use of bulkier triisopropylsilylcyclopentadiene (HCp<sup>TIPS</sup>) in this iGMM in diethyl ether led to crystallization of colorless blocks of [(Et<sub>2</sub>O)Mg(Cp<sup>TIPS</sup>)(μ-Br)]<sub>2</sub> (2) as depicted in Scheme 2. Complex 1 was moderately



**Scheme 2.** Synthesis of cyclopentadienylmagnesium bromide via the convenient in situ Grignard metalation method (iGMM).

soluble in ethereal solvents whereas the bulky triisopropylsilyl substituent in 2 significantly enhanced solubility in common organic solvents.

The asymmetric unit of dinuclear [(Et<sub>2</sub>O)Mg(Cp)(μ-Br)]<sub>2</sub> (1) contains a nearly centrosymmetric molecule A and half a molecule B that is completed by crystallographic inversion symmetry. Molecular structure and atom labeling scheme of molecule A are depicted in Figure 1, molecule B is shown in the Supporting Information. The magnesium atoms are in distorted tetrahedral environment with the largest angles of approx. 122° to the center of the Cp ligands (Cp<sub>cent</sub>-Mg-Br 121.4°–123.3°, Cp<sub>cent</sub>-Mg-O 121.0°–121.7°) and the smallest values for the endocyclic Br-Mg-Br bond angles (molecule A: 92.28(7)° and 91.84(7)°, B: 91.94(7)°).

Selected structural parameters of 1 are compared in Table 1 with the structures of [CpMg(Py)(μ-Br)]<sub>2</sub><sup>[9]</sup> and [CpMg(OEt<sub>2</sub>)(μ-Cl)]<sub>2</sub><sup>[11]</sup> to elucidate the influence of the halide and base strength of the coligand on the molecular structures. The central Mg<sub>2</sub>X<sub>2</sub> rings are nearly rectangular. In the pyridine adduct A the Mg-Br distances are very similar whereas in the complexes with bulkier diethyl ether ligands slightly different Mg-Br and Mg-Cl bond lengths are observed. The Mg-C bond lengths vary within a narrow range between 237.6 and 243.2 pm regardless of the coligands.

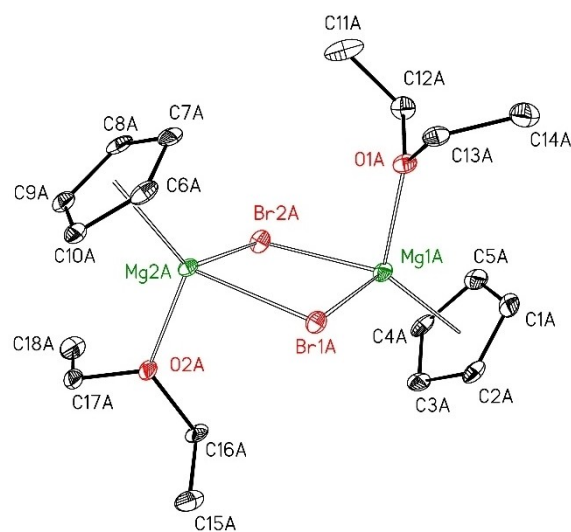


**Figure 1.** Molecular structure and atom labeling scheme of molecule A of dinuclear [(Et<sub>2</sub>O)Mg(Cp)(μ-Br)]<sub>2</sub> (1). The ellipsoids represent a probability of 30%, H atoms are omitted for clarity reasons.

**Table 1.** Comparison of selected structural parameters (average values, bond lengths [pm] and angles [deg.]) of  $[(Et_2O)Mg(Cp)(\mu-Br)]_2$  (**1**) with  $[CpMg(Py)(\mu-Br)]_2$ <sup>[9]</sup> (**A**) and  $[CpMg(OEt_2)(\mu-Cl)]_2$ <sup>[11]</sup> (**B**).

	1 A <sup>[a]</sup>	1 B <sup>[a]</sup>	A	B
Mg–X	258.4	257.8(2)	260.2(1)	241.9(2)
Mg–X'	260.3	260.9(2)	260.9(1)	243.2(2)
Mg–O/N	204.3	204.4(5)	215.5(2)	204.8(3)
Mg–C <sub>min</sub>	238.9	237.8(7)	239.3(5)	237.6(7)
Mg–C <sub>max</sub>	243.2	240.8(6)	242.5(3)	241.4(6)
Mg–X–Mg	87.38	88.06(7)	89.10(3)	89.90(5)
X–Mg–X	92.06	91.94(7)	90.90(3)	90.10(5)
O/N–Mg–C <sub>pcent</sub>	121.7	121.0	120.06	121.57
O/N–Mg–X	96.8	98.74(14)	94.66(7)	96.14(8)
O/N–Mg–X'	95.3	92.20(14)	98.04(7)	95.39(8)

[a] Molecule A and B of  $[(Et_2O)Mg(Cp)(\mu-Br)]_2$  (**1**).

Molecular structure and atom labeling scheme of dinuclear  $[(Et_2O)Mg(Cp^{TIPS})(\mu-Br)]_2$  (**2**) are depicted in Figure 2. The molecule contains a strictly planar four-membered  $Mg_2Br_2$  ring due to crystallographic inversion symmetry. The Mg1–Br1 and Mg1–Br1 A distances of 258.03(7) and 261.94(8) pm, respectively, differ by nearly 4 pm. The bulky triisopropylsilyl substituent slightly enhances the Mg1–O1 (206.92(16) pm) and Mg1–C<sub>Cp</sub> bond lengths (240.0(2) – 244.5(2) pm). Expectedly, the Si–C5 bond length of 187.2(2) pm to the  $sp^2$  hybridized carbon atom C5 is smaller than the distances to the  $sp^3$  hybridized carbon atoms of the isopropyl groups (189.9(2) to 190.7(2) pm).

The bulky triisopropylsilyl substituent leads to a slight slippage of the cyclopentadienide anion in complex **2**. Contrary to compound **1** with very similar  $Cp_{cent}$ –Mg1–Br1 and  $Cp_{cent}$ –Mg1–Br1A bond angles (molecule A: 121.4° and 122.2°; B: 122.0° and 123.3°), these values differ by 5.9° in complex **2** (119.6° and 125.5°). The O1–Mg–C<sub>pcent</sub> bond angle of 121.8° in **2** is very similar to the values of **1** verifying a rather small steric hindrance of the large triisopropylsilyl group.

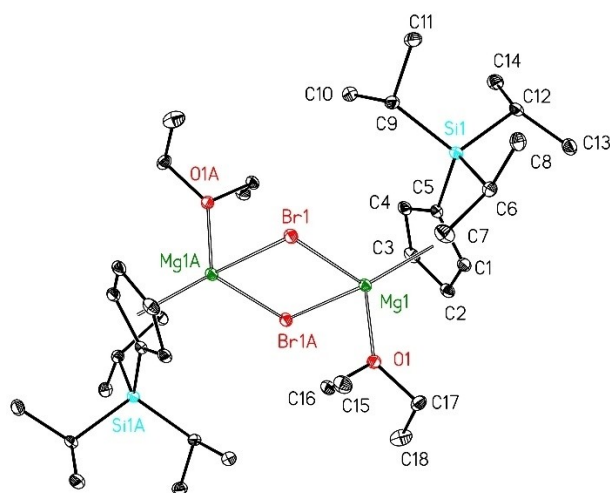
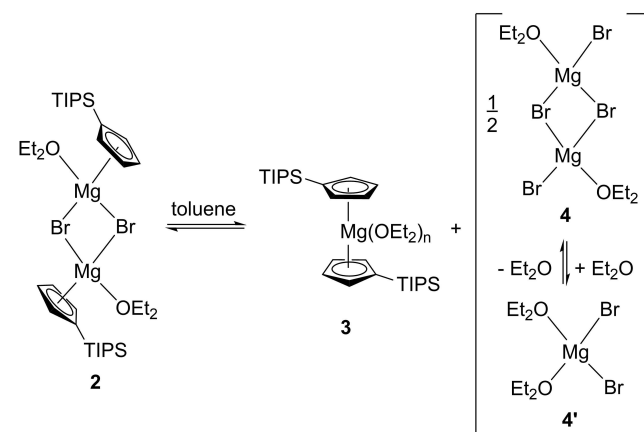


**Figure 2.** Molecular structure and atom labelling scheme of centrosymmetric dinuclear  $[(Et_2O)Mg(Cp^{TIPS})(\mu-Br)]_2$  (**2**). Symmetry-equivalent atoms ( $-x+1$ ,  $-y+1$ ,  $-z+2$ ) are marked with the letter A. The ellipsoids represent a probability of 30%, H atoms are neglected for clarity reasons.

DOSY NMR experiments in  $[D_8]$ toluene showed that a dinuclear structure of **2** is maintained in hydrocarbon solution. However, two sets of resonances with an intensity ratio of 1:0.57 was observed at 296 K suggesting an operative Schlenk equilibrium according to Scheme 3 yielding homoleptic  $[(Et_2O)Mg(Cp^{TIPS})_2]$  (**3-OEt<sub>2</sub>**, **3'**) and  $[(Et_2O)Mg(\mu-Br)]_2$  (**4**). DOSY NMR experiments in  $[D_8]$ toluene solution verified the adduct formation of **3** with diethyl ether. Crystallization of magnesium salt **4** from toluene led to the strand structure  $[(Et_2O)Mg(\mu-Br)]_2$  (**4**) in the solid state, however, solubility in hydrocarbon solution suggested deaggregation and an equilibrium with mono- and dinuclear species as depicted in Scheme 3. This equilibrium is strongly dependent on the temperature with increasing amounts of homoleptic  $[(Et_2O)Mg(Cp^{TIPS})_2]$  (**3'**) and magnesium bromide at increasing temperatures mainly caused by the entropic influence. The NMR spectroscopic study at a solution, prepared from crystalline  $[(Et_2O)Mg(Cp^{TIPS})(\mu-Br)]_2$  (**2**) in  $[D_8]$ toluene, revealed a molar ratio of **2**:**3'** of 1:1 at 253 K over 1:0.57 at 273 K to 1:0.28 at 323 K. Above 353 K homoleptic magnesocene **3'** is the dominating species in this solution. At room temperature, the chemical <sup>1</sup>H NMR shifts of  $\delta=3.77$  and 3.26 ppm for the methylene moieties of ligated diethyl ether molecules and uncoordinated free ether, respectively, can be distinguished (see Supporting Information). However, it is very challenging to estimate the influence of the limited amount of ethereal Lewis base on this Schlenk equilibrium because solvation-desolvation and aggregation-deaggregation equilibria interfere with the Schlenk-type ligand exchange reactions.

Crystallization of magnesium bromide from toluene with a limited amount of diethyl ether gave crystalline  $[(Et_2O)Mg(\mu-Br)]_2$  (**4**). Molecular structure and atom labeling scheme of (**4**) are depicted in Figure 3. The penta-coordinate magnesium centers are in distorted bipyramidal coordination environments with a linear arrangement of the Br1A–Mg1–Br2B moiety (178.59(10)°). The Mg1–Br1A and Mg1–Br2B bond lengths to the apical bromine atoms are significantly larger than those to the equatorial atoms Br1 and Br2. In agreement with the VSEPR model the apical anions experience a larger repulsion than the



**Scheme 3.** Schlenk-type equilibrium of  $[(Et_2O)Mg(Cp^{TIPS})(\mu-Br)]_2$  (**2**) in  $[D_8]$ toluene yielding homoleptic  $[(Et_2O)_nMg(Cp^{TIPS})_2]$  (**3**) and magnesium bromide with various ether contents (see text).

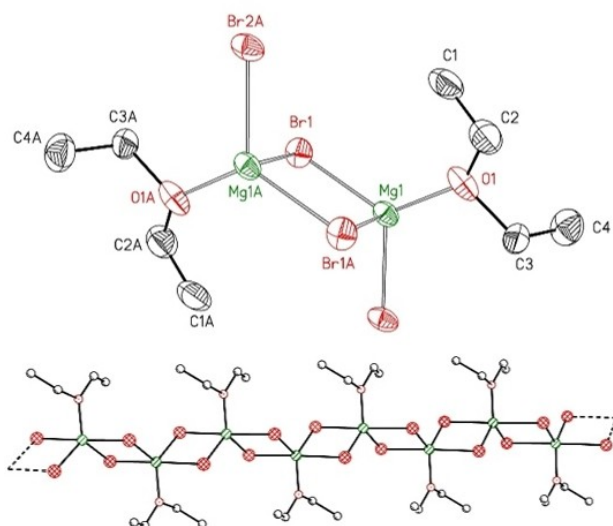


**Figure 3.** Molecular structure and atom labelling scheme of  $[(\text{Et}_2\text{O})\text{Mg}(\mu\text{-Br})_2]_\infty$  (**4**) are shown at the top. Symmetry-related atoms are marked by the letters A ( $-x, -y + 1, -z + 1$ ). The ellipsoids represent a probability of 30%, H atoms are omitted for the sake of clarity. Selected bond lengths (pm): Mg1-Br1 252.7(3), Mg1-Br2 252.5(2), Mg1-Br1A 267.6(2), Mg1-Br2B 268.0(2), Mg1-O1 199.5(6); angles (deg.): Br1-Mg1-Br2 119.56(10), Br1-Mg1-O1 124.6(2), Br1-Mg1-Br1A 88.55(8), Br1-Mg1-Br2B 92.08(8), Br2-Mg1-O1 115.8(2), Br2-Mg1-Br1A 92.54(8), Br2-Mg1-Br2B 88.25(8), O1-Mg1-Br1A 89.71(19), O1-Mg1-Br2B 88.90(18), Br1A-Mg1-Br2B 178.59(10). At the bottom, the strand structure with bridging bromine atoms is depicted.

equatorial atoms leading to enhanced Mg–Br distances. In a covalent picture (probably justified by an electronegativity difference  $\Delta\text{EN}$  of only 1.51 based on Allred-Rochow EN values for Mg and Br of 1.23 and 2.74),<sup>[25]</sup>  $\text{sp}^2$  hybridization can be assumed for Mg1 with bonds to the atoms Br1, Br2 and O1; perpendicular to this plane a 3-center 4-electron Br1A-Mg1-Br2B bond leads to a lower bond order between these atoms.

Larger coordination numbers than five seem to be feasible, too. Therefore, the alkyl groups have to direct to the periphery of the molecule which can be realized with cyclic ether ligands with a reduced degree of mobility of the O-bound alkyl groups. To verify this assumption, the structure of  $[(\text{thp})_4\text{MgBr}_2]$  (**5**) with unstrained cyclic tetrahydropyran (thp) was determined. Molecular structure and atom labeling scheme of molecule A of **5** are depicted in Figure 4, molecule B is shown in the Supporting Information. The enhanced coordination number of the magnesium atoms, which are in distorted octahedral environments, leads to an elongation of the Mg–O bonds and to rather large Mg–Br distances.

Differently solvated magnesium bromide and cyclopentadienyl magnesium bromide complexes as well as magnesocene molecules have been authenticated in solution and the solid state. To avoid equilibria between differently solvated species which make the quantitative analysis challenging, the investigation of the Schlenk equilibrium was repeated in a solvent mixture of diethyl ether and  $[\text{D}_8]$ toluene. This procedure allows to neglect solvation-desolvation and aggregation-deaggregation equilibria and to focus on the concentrations of the cyclopentadienyl magnesium species. A huge excess of Lewis

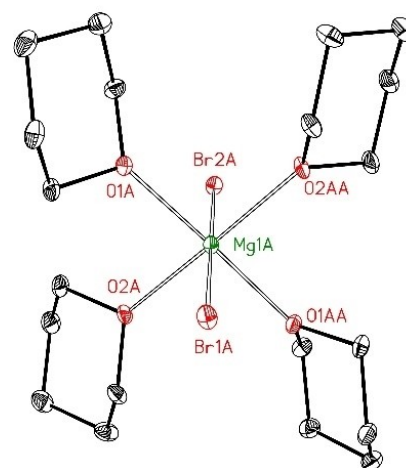
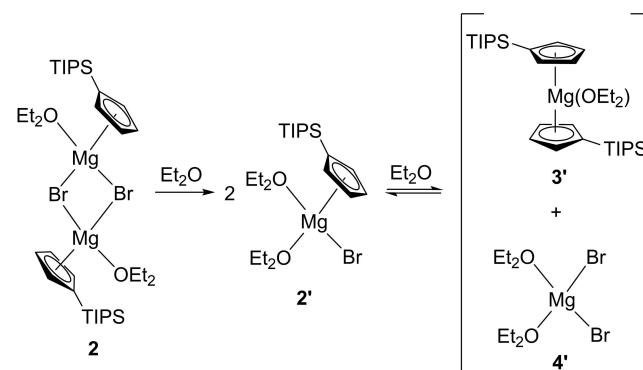


**Figure 4.** Molecular structure and atom labelling scheme of molecule A of  $[(\text{thp})_4\text{Mg}(\text{Br})_2]$  (**5**) is shown at the top. Symmetry-related atoms are marked by another letter A ( $-x-1, y, -z-0.5$ ). The ellipsoids represent a probability of 30%, H atoms are omitted for the sake of clarity. Selected bond lengths (pm): Mg1A-Br1A 267.51(18), Mg1A-Br2A 262.90(18), Mg1A-O1A 212.5(3), Mg1A-O2A 212.4(3); angles (deg.): Br1A-Mg1A-Br2A 180.0, Br1A-Mg1A-O1A 87.73(9), Br1A-Mg1A-O2A 92.07(9), Br2A-Mg1A-O1A 92.27(9), Br2A-Mg1A-O2A 87.93(9), O1A-Mg1A-O2A 88.68(10).

basic solvent leads to solvated mononuclear species and the amount of available free Lewis bases can be considered as constant. DOSY NMR experiments at 243 K in a solvent mixture of diethyl ether and  $[\text{D}_8]$ toluene verify the formation of the mononuclear bis(diethyl ether) adduct  $[(\text{Et}_2\text{O})_2\text{Mg}(\text{Cp}^{\text{TIPS}})\text{Br}]$  (**2'**). Thus the reaction partners of the Schlenk equilibrium simplify to the mononuclear species  $[(\text{Et}_2\text{O})_2\text{Mg}(\text{Cp}^{\text{TIPS}})\text{Br}]$  (**2'**),  $[(\text{Et}_2\text{O})\text{Mg}(\text{Cp}^{\text{TIPS}})_2]$  (**3'**) and  $[(\text{Et}_2\text{O})_2\text{MgBr}_2]$  (**4'**) with coordinative saturation of the magnesium centers by ethereal Lewis bases as depicted in Scheme 4.

With the knowledge of the mononuclear nature of the species involved in the Schlenk equilibrium, the temperature-dependency of the equilibrium constant allowed the determination of thermodynamic data (see Supporting Information). The reaction enthalpy  $\Delta\text{H}$  and reaction entropy  $\Delta\text{S}$  adopt



**Scheme 4.** Schlenk equilibrium of heteroleptic  $[(\text{Et}_2\text{O})_2\text{Mg}(\text{Cp}^{\text{TIPS}})\text{Br}]$  (**2'**) after dissolution of  $[(\text{Et}_2\text{O})\text{Mg}(\text{Cp}^{\text{TIPS}})(\mu\text{-Br})_2]$  (**2**) in diethyl ether involving only mononuclear  $\text{Et}_2\text{O}$  adducts of homoleptic  $\text{MgBr}_2$  and  $\text{Mg}(\text{Cp}^{\text{TIPS}})_2$ .

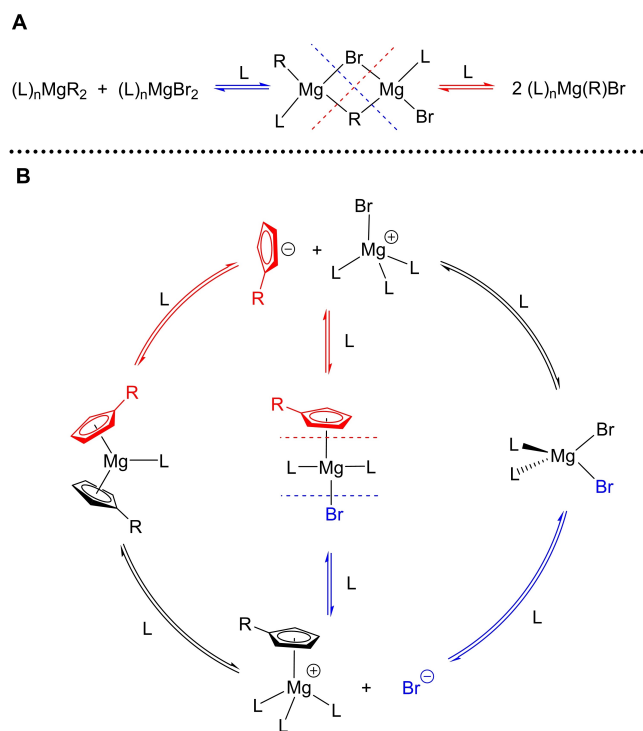
values of  $-11.5 \text{ kJ mol}^{-1}$  and  $60 \text{ J mol}^{-1}$ , respectively, and lie in the same order of magnitude as observed by NMR spectroscopy for ethereal solutions of selected aryl Grignard reagents (Table 2).<sup>[26]</sup> In diethyl ether arylmagnesium species are largely  $\text{ArMgX}$  and hence, neither reliable equilibrium constants nor thermodynamic parameters were available for the Schlenk equilibrium in this solvent.

Mechanistically, the Schlenk equilibrium can proceed via dimerization with bridging organyl and halide ligands, followed by deaggregation. This associative mechanism, commonly accepted for alkyl- and arylmagnesium Grignard reagents, can interconvert heteroleptic complexes into homoleptic congeners and *vice versa* as depicted at the top in Scheme 5. In the middle the heteroleptic and coordinatively saturated complex  $(\text{L})_2\text{MgCp}^*\text{Br}$  is depicted. Dissociation can now lead to the solvent-separated ion pairs  $[(\text{L})_n\text{MgBr}]^+ [\text{Cp}^*]^-$  (red arrows) or alternatively to  $[(\text{L})_n\text{MgCp}^*]^+ \text{Br}^-$  (blue arrows). Recombination

**Table 2.** Comparison of thermodynamic parameters  $\Delta H$  ( $\text{kJ mol}^{-1}$ ) and  $\Delta S$  ( $\text{J mol}^{-1}$ ) for the Schlenk equilibrium of Grignard reagents  $\text{RMgX}$ .<sup>[a]</sup>

RMgX	Solvent	$\Delta H$	$\Delta S$	Ref.
$[\text{3,5-D}_2]\text{PhMgBr}$	THF	+13.3	+56	[26]
$[\text{3,5-D}_2]\text{PhMgBr}$	2-MeTHF <sup>[b]</sup>	-10.6	-21	[26]
$2,6\text{-Me}_2\text{C}_6\text{H}_3\text{-MgBr}$	THF	+8.0	+56	[26]
$2\text{-F}_3\text{C-C}_6\text{H}_4\text{-MgBr}$	THF	0.0	+22	[26]
$2\text{-F}_3\text{C-C}_6\text{H}_4\text{-MgBr}$	2-MeTHF <sup>[b]</sup>	+13.5	+75	[26]
$(\text{Cp}^{\text{TIPS}})\text{MgBr}$ (2)	$\text{Et}_2\text{O}$	-11.5	+60	here

[a] All thermodynamic values have been determined by NMR spectroscopy. [b] 2-MeTHF = 2-methyltetrahydrofuran.



**Scheme 5.** Associative (A, at the top) and dissociative mechanism (B, at the bottom) for the Schlenk-type ligand exchange equilibrium interconverting homoleptic and heteroleptic magnesium complexes (see text).

of  $[(\text{L})_n\text{MgCp}^*]^+$  with  $[\text{Cp}^*]^-$  yields the magnesocene  $[(\text{L})\text{MgCp}^*]_2$  and also the bromide ion can bind to the bromomagnesium cations giving  $[(\text{L})_2\text{MgBr}_2]$ . The red color shows the transferred  $\text{Cp}^*$  ligand, the blue color the transferred bromide ion.

Contrary to this mechanism, cyclopentadienyl anions in bridging positions between magnesium atoms are unknown. Therefore, an associative mechanism has been rejected to explain the experimental findings. Dissociation of  $[(\text{L})_n\text{Mg}(\text{Cp}^{\text{R}})\text{Br}]$  in Lewis basic solvents L yields either  $[(\text{L})_n\text{Mg}(\text{Cp}^{\text{R}})]^+$  and bromide ions or  $[(\text{L})_n\text{MgBr}]^+$  and  $(\text{Cp}^{\text{R}})^-$  anions as shown in the bottom part of Scheme 5. Both cations can bind either bromide or cyclopentadienide anions leading to hetero- and homoleptic magnesium complexes. Formation of earlier observed anionic species such as  $[(\text{L})_n\text{MgBr}_3]^-$  and probably even  $[\text{MgBr}_4]^{2-}$  seem feasible via additional exchange of ligated solvent molecules by bromide ions and can easily be explained by the proposed dissociative mechanism. This explanation is strongly supported by the observed low conductivity of ethereal magnesocene solutions.<sup>[5]</sup>

## Conclusions

The direct metalation of H-acidic compounds (such as amines and cyclopentadienes) with magnesium metal is impossible due to the large ionization potentials compared to the alkali and heavy alkaline-earth metals. Therefore, a multiple-step protocol had to be chosen including the preparation of a Grignard reagent, titration of the ethereal Grignard solution and adjusting the exact stoichiometry of the substrates  $\text{RMgX}$  and  $\text{Cp}^{\text{R}}\text{H}$ . The innovative *in situ* Grignard metalation method (iGMM) allows the straightforward synthesis of unsubstituted and substituted cyclopentadienyl magnesium bromides with a beneficial one-pot procedure. The addition of bromoethane to a suspension of magnesium turnings and cyclopentadienes in ethereal solvents smoothly leads to the formation of ether adducts of cyclopentadienyl magnesium bromides. Cooling of these Grignard solutions leads to dinuclear  $[(\text{Et}_2\text{O})\text{Mg}(\text{Cp}^{\text{R}})(\mu\text{-Br})_2]$  ( $\text{R}=\text{H}$  (1),  $\text{Si}(i\text{Pr})_3$  (TIPS, 2) with central four-membered  $\text{Mg}_2\text{Br}_2$  rings. Temperature-dependent Schlenk equilibria in toluene convert these complexes into the homoleptic congeners, namely magnesocene  $\text{Mg}(\text{Cp}^{\text{R}})_2$  (3) and magnesium bromide  $[(\text{Et}_2\text{O})\text{Mg}(\text{Br})(\mu\text{-Br})_2]$  (4).

To circumvent interference of solvation-desolvation and aggregation-deaggregation equilibria with Schlenk-type ligand redistribution reactions, thermodynamic parameters have been elucidated at ethereal solutions of  $[(\text{Et}_2\text{O})\text{Mg}(\text{Cp}^{\text{TIPS}})(\mu\text{-Br})_2]$  (2). DOSY NMR experiments in a solvent mixture of diethyl ether and  $[\text{D}_8]\text{toluene}$  verify the mononuclear appearance of  $[(\text{Et}_2\text{O})_2\text{Mg}(\text{Cp}^{\text{TIPS}})\text{Br}]$  (2'),  $[(\text{Et}_2\text{O})\text{Mg}(\text{Cp}^{\text{TIPS}})_2]$  (3'), and  $[(\text{Et}_2\text{O})_2\text{MgBr}_2]$  (4') that are interconnected by a temperature-dependent Schlenk-type equilibrium. The temperature dependency of the equilibrium constant allows the determination of a reaction enthalpy  $\Delta H$  of  $-11.5 \text{ kJ mol}^{-1}$  and a reaction entropy  $\Delta S$  of  $60 \text{ J mol}^{-1}$ .

In summary, we could develop a simple procedure for the preparation of cyclopentadienyl-based Grignard solutions. Fur-

thermore, a quantitative elucidation of thermodynamic data by NMR experiments succeeded based on a temperature-dependent Schlenk-type equilibrium via a dissociative ligand exchange mechanism.

## Experimental Section

**General Information:** All manipulations were carried out under an inert nitrogen atmosphere using standard Schlenk techniques, if not otherwise noted. The solvents were dried over KOH and subsequently distilled over sodium/benzophenone under a nitrogen atmosphere prior to use. All substrates were purchased from Alfa Aesar, abcr, Sigma Aldrich or TCI and used without further purification. Cyclopentadiene was freshly distilled from dicyclopentadiene and copper powder at 160 °C. The yields given are not optimized. Purity of the compounds was verified by NMR spectroscopy. Deuterated solvents were dried over sodium, distilled, degassed, and stored under nitrogen over sodium.  $^1\text{H}$ ,  $^{25}\text{Mg}$ ,  $^{29}\text{Si}$  and  $^{13}\text{C}\{^1\text{H}\}$  NMR spectra were recorded on Bruker Avance III 400 (BBO, BBFO probes), Avance II HD 500 (BBO Prodigy probe) or Avance neo 500 (BBFO Prodigy probe) spectrometers. Chemical shifts are reported in parts per million relatively to  $\text{SiMe}_4$  as an external standard referenced to the solvents residual proton signal using *xiref* AU program for  $^{13}\text{C}$ ,  $^{25}\text{Mg}$ ,  $^{29}\text{Si}$  NMR spectra.  $^{25}\text{Mg}$  NMR was recorded using the *aring* pulse sequence and 20.000–100.000 scans ( $D1=0.05$  s). DOSY NMRs were measured using the convection compensated *dsteppgp3* standard pulse sequence (64 increments,  $\Delta=0.75$  s,  $\delta=2.5$  ms). Molar masses in solution were calculated using the *Stalke*-ECC-DOSY method (standard: adamantane or  $\text{Si}(\text{SiMe}_3)_4$ ).<sup>[27]</sup> ASAP-HSQC-spectra and ASAP-HSQC-DEPT-spectra were recorded using the published pulse sequences.<sup>[28]</sup>  $\text{Cp}^{\text{TIPS}}\text{H}$  was prepared according to a slightly modified literature procedure.<sup>[29]</sup> The elemental analyses of the magnesium complexes gave no reliable results due to loss of ligated ether ligands during handling and combustion. The silicon-containing compounds gave low carbon values due to formation of silicon carbide.

**Synthesis of  $\text{C}_5\text{H}_5\text{-Si}(\text{iPr})_3$  ( $\text{Cp}^{\text{TIPS}}\text{H}$ ):** Chloro-triisopropylsilane (TIPS-Cl, 19.3 g, 100 mmol, 1 equiv.) was added at room temperature to a NaCp solution (0.5 M in THF, 200 mL, 100 mmol, 1 equiv.). The reaction mixture was stirred for 24 h at room temperature. Water (200 mL) was added, the organic layer was separated, and the aqueous layer was washed with  $\text{Et}_2\text{O}$  ( $3 \times 100$  mL). The combined organic layers were dried with anhydrous  $\text{MgSO}_4$  and the solvents were removed under reduced pressure. The residue was fractionally distilled using a short *Vigreux* column yielding 11.6 g of  $\text{Cp}^{\text{TIPS}}\text{H}$  as slightly yellow oil (52 mmol, 52%) and 7.4 g of  $\text{C}_5\text{H}_4\text{-1,3-[Si}(\text{iPr})_2\text{Cp}^{\text{TIPS}}\text{H}$  (20 mmol, 39%) as orange viscous oil.

**Physical data of  $\text{C}_5\text{H}_5\text{-Si}(\text{iPr})_3$  ( $\text{HCp}^{\text{TIPS}}$ ):** Sdp: 45 °C /  $1.3 \times 10^{-2}$  mbar. IR (ATR)  $\nu=2941$  (m), 2890 (w), 2864 (s), 1462 (m), 918 (s), 670 (s), 647 (s)  $\text{cm}^{-1}$ .  $^1\text{H}$  NMR (400 MHz,  $\text{CDCl}_3$ , 297 K):  $\delta=6.84$ - $6.39$  (m, 4H, CH-Cp), 3.48 (br, 0.4H,  $\text{CH}_2$ -Cp), 3.04 (q,  $J=1.45$  Hz, 1.1H,  $\text{CH}_2$ -Cp), 2.99 (q,  $J=1.55$  Hz, 0.5H,  $\text{CH}_2$ -Cp), 1.26-1.04 (m, 3H, TIPS-CH), 1.01 (m, 24H, TIPS- $\text{CH}_3$ ).  $^{13}\text{C}\{^1\text{H}\}$  NMR (125 MHz,  $\text{CDCl}_3$ , 297 K):  $\delta=144.8$ , 143.7, 142.5, 140.8, 137.5, 136.9, 134.3 (br), 132.8, 131.8, 130.2, 47.3, 47.1, 43.6, 19.0, 18.77, 18.71, 12.5, 12.3, 11.6, 11.2 ppm.  $^{29}\text{Si}\{^1\text{H}\}$  NMR (99.4 MHz,  $\text{CDCl}_3$ , 297 K):  $\delta=9.7$ ,  $-1.5$ ,  $-1.6$  ppm. MS (EI+)  $e/z=379$  [M] $^+$ .

**Physical data of  $\text{C}_5\text{H}_5\text{-1,3-[Si}(\text{iPr})_2\text{Cp}^{\text{TIPS}}\text{H}$  ( $\text{HCp}^{2\text{TIPS}}$ ):** ( $^{29}\text{Si}$  and  $^{13}\text{C}$  shifts of TIPS group can not assigned to the isomers) Sdp: 143 °C /  $1.3 \times 10^{-2}$  mbar. IR (ATR)  $\nu=2941$  (m), 2890 (w), 2864 (s), 1462 (m), 1074 (m), 918 (s), 670 (s), 647 (s)  $\text{cm}^{-1}$ .  $^{29}\text{Si}\{^1\text{H}\}$  NMR (99.4 MHz,  $\text{CDCl}_3$ , 297 K):  $\delta=9.8$ , 4.9,  $-1.52$ ,  $-1.57$ ,  $-1.68$ ,  $-2.0$  ppm.  $^{13}\text{C}\{^1\text{H}\}$  NMR (125 MHz,  $\text{CDCl}_3$ , 297 K, TIPS groups):  $\delta=19.14$ , 19.11, 18.8, 17.7,

13.4, 12.4, 11.62, 11.56, 11.38, 11.22 ppm. MS (EI+)  $e/z=222.18$  [M] $^+$ . **Isomer A:**  $^1\text{H}$  NMR (500 MHz,  $\text{CDCl}_3$ , 297 K):  $\delta=6.94$  (t,  $J=1.6$  Hz, 1H), 6.67 (br, 2H), 3.60 (br, 1H), 1.22 (m, 6H), 1.06 (m, 36H) ppm.  $^{13}\text{C}\{^1\text{H}\}$  NMR (125 MHz,  $\text{CDCl}_3$ , 297 K):  $\delta=143.9$ , 133.3, 135.5, 49.2 ppm. **Isomer B:**  $^1\text{H}$  NMR (500 MHz,  $\text{CDCl}_3$ , 297 K):  $\delta=6.92$  (br, 2H), 3.15 (t,  $J=1.4$  Hz, 2H), 1.22 (m, 6H), 1.06 (m, 36H) ppm.  $^{13}\text{C}\{^1\text{H}\}$  NMR (125 MHz,  $\text{CDCl}_3$ , 297 K):  $\delta=145.6$ , 49.2 ppm. **Isomer C:**  $^1\text{H}$  NMR (500 MHz,  $\text{CDCl}_3$ , 297 K):  $\delta=6.91$  (q,  $J=1.1$  Hz, 1H), 6.89 (q,  $J=1.5$  Hz, 1H), 3.17 (t,  $J=1.5$  Hz, 2H), 1.22 (m, 6H), 1.06 (m, 36H) ppm.  $^{13}\text{C}\{^1\text{H}\}$  NMR (125 MHz,  $\text{CDCl}_3$ , 297 K):  $\delta=148.9$ , 148.6, 52.8 ppm.

**Synthesis of  $[(\text{Et}_2\text{O})\text{Mg}(\text{Cp})\text{Br}]_\infty$  (1):** Magnesium turnings (1.0 g, 41 mmol, 1.1 equiv.) and freshly distilled CpH (3.4 mL, 37 mmol, 1 equiv.) was suspended in 25 mL of  $\text{Et}_2\text{O}$ . The mixture was cooled to 0 °C and EtBr (3.1 mL, 41 mmol, 1.1 equiv.) was added in three portions. After 30 min at 0 °C the reaction mixture was warmed to room temperature and decanted from the residual magnesium turnings. The clear greyish solution was stored at room temperature for 2 days. The crystalline precipitate was separated by filtration and carefully dried under reduced pressure.  $[(\text{Et}_2\text{O})\text{Mg}(\text{Cp})\text{Br}]_\infty$  was obtained as large colorless blocks (5.7 g, 11.7 mmol, 57%).  $^1\text{H}$  NMR (400 MHz,  $[\text{D}_8]\text{toluene}$ , 297 K):  $\delta=6.32$  (br, 10H, Cp), 3.85 (8H, q,  $J=6.3$  Hz,  $\text{Et}_2\text{O}$ ), 0.92 (12H, t,  $J=6.3$  Hz,  $\text{Et}_2\text{O}$ ).  $^{13}\text{C}\{^1\text{H}\}$  NMR (101 MHz,  $[\text{D}_8]\text{toluene}$ , 297 K):  $\delta=106.1$  (Cp), 64.9 ( $\text{Et}_2\text{O}$ ), 13.3 ( $\text{Et}_2\text{O}$ ).  $^{25}\text{Mg}$  NMR (24.5 MHz,  $[\text{D}_8]\text{toluene}$ , 297 K)  $\delta=-43$ .

**Synthesis of  $(\text{thf})_n\text{Mg}(\text{Cp})\text{Br}$ .** Magnesium turnings (1.0 g, 41 mmol, 1.1 equiv.) and freshly distilled HCp (3.4 mL, 37 mmol, 1 equiv.) were suspended in 30 mL of THF. The mixture was cooled to 0 °C and EtBr (3.1 mL, 41 mmol, 1.1 equiv.) was added in three portions. After 30 min at 0 °C the reaction mixture was warmed to room temperature and decanted from the residual magnesium turnings. Titration of a hydrolyzed aliquot with sulfuric acid against phenolphthalein showed a conversion of 74%. The solvent was removed leaving a highly viscous oily residue.  $^1\text{H}$  NMR (400 MHz,  $[\text{D}_8]\text{toluene}$ , 297 K):  $\delta=6.24$  (s, 5H, Cp), 3.60 (m, 20H, thf), 1.49 (m, 20H, thf).  $^{13}\text{C}\{^1\text{H}\}$  NMR (101 MHz,  $[\text{D}_8]\text{toluene}$ , 297 K):  $\delta=105.0$  (Cp), 68.6 (thf), 25.1 (thf).  $^{25}\text{Mg}$  NMR (24.5 MHz,  $[\text{D}_8]\text{toluene}$ , 297 K)  $\delta=18$  (0.17, (thf) $\text{MgBr}_2$ ),  $-32$  (1.0, [(thf) $\text{Mg}(\text{Cp})\text{Br}]_n$ ).

**Synthesis of  $[(\text{Et}_2\text{O})\text{Mg}(\text{Cp}^{\text{TIPS}})\text{Br}]_2$  (2):** Magnesium turnings (100 mg, 4.1 mmol, 1.1 equiv.) and freshly distilled  $\text{Cp}^{\text{TIPS}}\text{H}$  (830 mg, 3.7 mmol, 1 equiv.) were suspended in  $\text{Et}_2\text{O}$  (4.1 mL). The mixture was cooled to 0 °C and EtBr (280  $\mu\text{L}$ , 3.7 mmol, 1 equiv.) was added in three portions. After 3 h at 0 °C the reaction mixture was warmed to room temperature and decanted from the residual magnesium turnings. The clear, slightly yellow solution was stored at room temperature for 48 h. The crystalline precipitate was separated by filtration and carefully dried under reduced pressure.  $[(\text{Et}_2\text{O})\text{Mg}(\text{Cp}^{\text{TIPS}})\text{Br}]_2$  (2) was obtained as large colorless blocks (895 mg, 1.12 mmol, 60%). In toluene solution, a Schlenk equilibrium was observed leading to a mixture of 2, magnesocene 3 and magnesium bromide (see text).  $^1\text{H}$  NMR (400 MHz,  $[\text{D}_8]\text{toluene}$ , 297 K):  $\delta=6.39$  (br, 2H, Cp(2)), 6.26 (br, 2H, Cp(2)), 6.09 (m, 2H, Cp(3)), 6.07 (m, 2H, Cp(3)), 3.19 (br, 4H,  $\text{Et}_2\text{O}$ ), 1.23-1.09 (m, 3H, TIPS(2)), 1.03-0.92 (m, 18H, TIPS(2)), 1.00-0.90 (m, 3H, TIPS(3)), 0.90-0.82 (m, 18H, TIPS(3)), 0.78 (t, 6H,  $J=7.0$  Hz,  $\text{Et}_2\text{O}$ ).  $^1\text{H}$ -DOSY NMR (400 MHz,  $[\text{D}_8]\text{toluene}$ , 297 K):  $D([\text{D}_7]\text{toluene})=2.24 \times 10^{-9}$   $\text{m}^2/\text{s}$ ,  $D(\text{substance})=6.1 \times 10^{-10}$   $\text{m}^2/\text{s}$ , MW(calc,  $[(\text{Et}_2\text{O})\text{Mg}(\text{Cp}^{\text{TIPS}})\text{Br}]_2$ ) = 830 g/mol, MW(found) = 811 g/mol,  $\Delta=2\%$ ;  $D(\text{Tol-d}_7)=2.24 \times 10^{-9}$   $\text{m}^2/\text{s}$ ,  $D(\text{Subst.})=7.7 \times 10^{-10}$   $\text{m}^2/\text{s}$ , MW: calc. for  $[(\text{Et}_2\text{O})\text{Mg}(\text{Cp}^{\text{TIPS}})]_2$ : 540 g/mol, found: 550 g/mol,  $\Delta=-2\%$ .  $^{13}\text{C}\{^1\text{H}\}$  NMR (101 MHz,  $[\text{D}_8]\text{toluene}$ , 297 K):  $\delta=116.7$  (Cp $^{\text{TIPS}}$ (3)), 116.3 (Cp $^{\text{TIPS}}$ (2)), 111.9 (Cp $^{\text{TIPS}}$ (2)), 110.6 (Cp $^{\text{TIPS}}$ (3)), 108.7, 65.2 ( $\text{Et}_2\text{O}$ ), 19.3 (TIPS(2)), 18.8 (TIPS(3)), 13.9 ( $\text{Et}_2\text{O}$ ), 12.3 (TIPS(2)), 11.5 (TIPS(3)) ppm.  $^{29}\text{Si}$  NMR (78.5 MHz,  $[\text{D}_8]\text{toluene}$ , 297 K):  $\delta=-0.95$  (3),  $-1.71$  (2).

**Synthesis of [(Et<sub>2</sub>O)MgBr<sub>2</sub>]<sub>2</sub>:** Magnesium turnings (1 g, 41 mmol, 1 equiv.) were suspended in Et<sub>2</sub>O (40 mL) and 1,2-dibromoethane (3.6 mL, 41 mmol, 1 equiv.) was added in four portions over 1 h. After complete addition the reaction mixture was heated to reflux for 30 min. The solvent was removed under reduced pressure. [(Et<sub>2</sub>O)MgBr<sub>2</sub>]<sub>2</sub> was obtained as colorless powder (10.6 g, quant., 20.5 mmol). The halogen content was determined by argentometric titration (0.05 M AgNO<sub>3</sub>) of a definite sample [m = 1.9 mg, c(Br<sup>-</sup> calc.) = 14.5 μmol, c(Br<sup>-</sup> found.) = 17 μmol]. Suitable crystals for X-Ray analysis were grown from a saturated toluene solution at room temperature.

**Crystal Structure determinations:** The intensity data for the compounds were collected on a Nonius KappaCCD diffractometer using graphite-monochromated Mo-K<sub>α</sub> radiation. Data were corrected for Lorentz and polarization effects; absorption was taken into account on a semi-empirical basis using multiple-scans.<sup>[30–32]</sup> The structures were solved by intrinsic phases (SHELXT)<sup>[33]</sup> and refined by full-matrix least squares techniques against F<sub>o</sub><sup>2</sup>.<sup>[34]</sup> All hydrogen atoms were included at calculated positions with fixed thermal parameters. All non-hydrogen atoms were refined anisotropically.<sup>[34]</sup> Crystallographic data as well as structure solution and refinement details are summarized in Table S1. The program packages XP<sup>[35]</sup> and POV-Ray<sup>[36]</sup> were used for structure representations.

## Supporting Information

NMR spectra, crystallographic and refinement details, molecular representations of molecules B of complexes **1** and **5** (pdf format). Deposition Number(s) 2092831 for **1**, 2092832 for **2**, 2092833 for **4**, and 866609 for **5** contain(s) the supplementary crystallographic data for this paper. These data are provided free of charge by the joint Cambridge Crystallographic Data Centre and Fachinformationszentrum Karlsruhe Access Structures service.

## Acknowledgements

We acknowledge the valuable support of the NMR service platform ([www.nmr.uni-jena.de/](http://www.nmr.uni-jena.de/)) of the Faculty of Chemistry and Earth Sciences of the Friedrich Schiller University Jena, Germany. Parts of the equipment were provided by the German Research Foundation (DFG, INST 275/442-1 FUGG) which we kindly acknowledge. P. Schüler is very grateful to the German Environment Foundation (Deutsche Bundesstiftung Umwelt, DBU, grant no. 20018/578) for a generous Ph.D. grant. The single crystal of **5** was provided by Dr. M. Köhler. Open Access funding enabled and organized by Projekt DEAL.

## Conflict of Interest

The authors declare no conflict of interest.

**Keywords:** cyclopentadienylmagnesium bromides · Grignard reagents · magnesocene · organomagnesium complexes · Schlenk equilibrium

- [1] Reviews on s-block metallocenes: a) P. Jutzi, *J. Organomet. Chem.* **1990**, *400*, 1–17; b) T. P. Hanusa, *Chem. Rev.* **1993**, *93*, 1023–1036; c) D. J. Burkey, T. P. Hanusa, *Comments Inorg. Chem.* **1995**, *17*, 41–77; d) I. Bytheway, P. L. A. Popelier, R. J. Gillespie, *Can. J. Chem.* **1996**, *74*, 1059–1071; e) A. J. Bridgeman, *J. Chem. Soc. Dalton Trans.* **1997**, 2887–2893; f) S. Harder, *Coord. Chem. Rev.* **1998**, *176*, 17–66; *ibid.* **2000**, *199*, 331–334 (corrigendum); g) P. Jutzi, N. Burford, *Chem. Rev.* **1999**, *99*, 969–990; h) P. Jutzi, G. Reumann, *J. Chem. Soc. Dalton Trans.* **2000**, 2237–2244; i) T. P. Hanusa, *Organometallics* **2002**, *21*, 2559–2571; j) P. H. M. Budzelaar, J. J. Engelberts, J. H. van Lenthe, *Organometallics* **2003**, *22*, 1562–1576; k) E. Cerpa, F. J. Tenorio, M. Contreras, M. Villanueva, H. I. Beltrán, T. Heine, K. J. Donald, G. Merino, *Organometallics* **2008**, *27*, 827–833.
- [2] C. Elschenbroich: *Organometallics*, 3<sup>rd</sup> ed., Wiley-VCH, Weinheim, **2006**, pp. 65–66.
- [3] B. J. Wakefield: *Organomagnesium Methods in Organic Synthesis*, Academic Press, London, **1995**, chap. 3, pp. 21–45.
- [4] J. Muldoon, C. B. Bucur, T. Gregory, *Chem. Rev.* **2014**, *114*, 11683–11720.
- [5] R. Schwarz, M. Pejic, P. Fischer, M. Marinaro, L. Jörissen, M. Wachtler, *Angew. Chem. Int. Ed.* **2016**, *55*, 14958–14962; *Angew. Chem.* **2016**, *128*, 15182–15186.
- [6] a) R. Benn, H. Lehmkuhl, K. Mehler, A. Ruffinska, *Angew. Chem. Int. Ed. Engl.* **1984**, *23*, 534–535; *Angew. Chem.* **1984**, *96*, 521–523. b) H. Lehmkuhl, K. Mehler, R. Benn, A. Ruffinska, C. Krüger, *Chem. Ber.* **1986**, *119*, 1054–1069; c) R. Benn, A. Ruffinska, *Angew. Chem. Int. Ed. Engl.* **1986**, *25*, 861–881; *Angew. Chem.* **1986**, *98*, 851–871.
- [7] C. P. Morley, P. Jutzi, C. Krüger, J. M. Wallis, *Organometallics* **1987**, *6*, 1084–1090.
- [8] M. Huber, H. Schnöckel, *Inorg. Chim. Acta* **2008**, *361*, 457–461.
- [9] T. Duan, H. Schnöckel, private CSD communication REVNOW, **2005**.
- [10] T. Duan, H. Schnöckel, private CSD communication REVNIQ, **2005**.
- [11] C. Dohmeier, D. Loos, C. Robl, H. Schnöckel, D. Fenske, *J. Organomet. Chem.* **1993**, *448*, 5–8.
- [12] a) R. Sarma, F. Ramirez, B. McKeever, Y. F. Chaw, J. F. Marecek, D. Nierman, T. M. McCaffrey, *J. Am. Chem. Soc.* **1977**, *99*, 5289–5295; b) R. E. Marsh, D. A. Clemente, *Inorg. Chim. Acta* **2007**, *360*, 4017–4024.
- [13] P. C. Andrews, M. Brym, C. Jones, P. C. Junk, M. Kloth, *Inorg. Chim. Acta* **2006**, *359*, 355–363.
- [14] a) M.-C. Pérucaud, M.-T. Le Bihan, *Acta Crystallogr.* **1968**, *B24*, 1502–1505; b) N. Metzler, H. Nöth, M. Schmidt, A. Treitl, *Z. Naturforsch.* **1994**, *49b*, 1448–1452; c) A. Lorbach, H.-W. Lerner, M. Bolte, *Acta Crystallogr.* **2007**, *C63*, m174; d) D. Stern, M. Granitzka, T. Schulz, D. Stalke, *Z. Naturforsch.* **2010**, *65b*, 719–724; e) J. W. Clary, T. J. Rettenmaier, R. Snelling, W. Bryks, J. Banwell, W. T. Wipke, B. Singaram, *J. Org. Chem.* **2011**, *76*, 9602–9610.
- [15] S. B. Munoz, S. L. Daifuku, W. W. Brennessel, M. L. Neidig, *J. Am. Chem. Soc.* **2016**, *138*, 7492–7495.
- [16] a) M. T. Caudle, W. W. Brennessel, V. G. Young, *Inorg. Chem.* **2005**, *44*, 3233–3240; b) C. Saalfrank, F. Fantuzzi, T. Kupfer, B. Ritschel, K. Hammond, I. Krummenacher, R. Bertermann, R. Wirthensohn, M. Finze, P. Schmid, V. Engel, B. Engels, H. Braunschweig, *Angew. Chem. Int. Ed.* **2020**, *59*, 19338–19343; *Angew. Chem.* **2020**, *132*, 19502–19507.
- [17] a) L. M. Guard, N. Hazari, *Organometallics* **2013**, *32*, 2787–2794; b) J. Peña, G. Talavera, B. Waldecker, M. Alcarazo, *Chem. Eur. J.* **2017**, *23*, 75–78.
- [18] H. Schibilla, M.-T. Le Bihan, *Acta Crystallogr.* **1967**, *23*, 332–333.
- [19] D. Y. Kim, Y. Yang, J. R. Abelson, G. S. Girolami, *Inorg. Chem.* **2007**, *46*, 9060–9066.
- [20] A. Jaenschke, J. Paap, U. Behrens, *Organometallics* **2003**, *22*, 1167–1169.
- [21] A. Jaenschke, F. Olbrich, U. Behrens, *Z. Anorg. Allg. Chem.* **2009**, *635*, 2550–2557.
- [22] U. Behrens, E. A. Dimos, *Z. Kristallogr.* **2012**, *227*, 509–510.
- [23] C. Müller, J. Warken, V. Huch, B. Morgenstern, I.-A. Bischoff, M. Zimmer, A. Schäfer, *Chem. Eur. J.* **2021**, *27*, 6500–6510.
- [24] S. Kriech, P. Schüler, J. M. Peschel, M. Westerhausen, *Synthesis* **2019**, *51*, 1115–1122.
- [25] A. F. Holleman, E. Wiberg, N. Wiberg: *Lehrbuch der Anorganischen Chemie*, Walter de Gruyter, Berlin, **2007**.
- [26] D. F. Evans, G. V. Fazakerley, *J. Chem. Soc. A* **1971**, 184–189.
- [27] R. Neufeld, D. Stalke, *Chem. Sci.* **2015**, *6*, 3354–3364.
- [28] a) D. Schulze-Sünninghausen, J. Becker, M. R. M. Koos, B. Luy, *J. Magn. Reson.* **2017**, *281*, 151–161; b) D. Schulze-Sünninghausen, J. Becker, B. Luy, *J. Am. Chem. Soc.* **2014**, *136*, 1242–1245.
- [29] R. Kränzle: *Synthese, Charakterisierung und Anwendung von neuen Alkalimetall- und Erdalkalimetallcyclopentadieniden*, Ph.D. Thesis, LMU Munich, **2005**.

- [30] R. Hoof: COLLECT, Data Collection Software; Nonius B. V., Netherlands, **1998**.
- [31] Z. Otwinowski, W. Minor, in *Methods Enzymol.* (Eds. C. W. Carter, R. M. Sweet), Vol. 276, part A, Academic Press, San Diego, USA, **1997**, pp. 307–326.
- [32] a) SADABS 2.10, Bruker-AXS Inc., Madison, WI, USA, **2002**; b) SADABS 2016/2: L. Krause, R. Herbst-Irmer, G. M. Sheldrick, D. Stalke, *J. Appl. Crystallogr.* **2015**, *48*, 3–10.
- [33] G. M. Sheldrick, *Acta Crystallogr.* **2015**, *C71*, 3–8.
- [34] A. L. Spek, *Acta Crystallogr.* **2015**, *C71*, 9–18.
- [35] XP, Siemens Analytical X-ray Instruments Inc., Karlsruhe, Germany, **1990**; Madison, WI, USA, **1994**.
- [36] POV-Ray, Persistence of Vision Raytracer, Victoria, Australia, **2007**.

---

Manuscript received: July 20, 2021

Accepted manuscript online: September 1, 2021

Version of record online: October 5, 2021